GMR
The Original

DESIGN, SYNTHESIS, AND *IN VITRO* SCREENING OF MACROCYCLIC UREA-BASED HETEROCYCLIC SYSTEMS WITH UNUSUAL RING CONSTRAINTS

Pradeep Kumar M.R. [1], Palati Divya Jyothi [2], G. Hemalatha [3], Mohit Kumar [4], Joel Mart E [5], Mayble Mary Lyngkhoi [6], Nikita Vilas Thorat [7], Prakhar Nema [8]*

[1.] Assistant Professor, KLE College of Pharmacy, KLE Academy of Higher Education and Research (KAHER), Vidyanagar, Hubballi, Karnataka 580031, India.
[2.] Associate Professor, Department of Pharmacognosy, School of Pharmacy, SBV Karaikal Campus, Sri Balaji Vidyapeeth (Deemed to be University), Karaikal, Puducherry 607403, India.
[3.] Professor, Telangana Social Welfare Residential Pharmacy College for Women, Mahabubabad, Telangana 506101, India.
[4.] Assistant Professor, Teerthanker Mahaveer College of Pharmacy, Teerthanker Mahaveer University, Delhi Road, Moradabad, Uttar Pradesh 244001, India.
[5.] Assistant Professor, Vels Institute of Science, Technology & Advanced Studies (VISTAS), Velan Nagar, P.V. Vaithiyalingam Road, Pallavaram, Chennai, Tamil Nadu 600117, India.
[6.] Assistant Professor, Department of Pharmacy, University of Science and Technology Meghalaya, Kling Road, Baridua, Ri Bhoi District, Meghalaya 793101, India.
[7.] Assistant Professor, College of Pharmaceutical Sciences, Pravara Institute of Medical Sciences (Deemed to be University), Loni BK, Taluka Rahata, Ahilyanagar (Ahmednagar), Maharashtra 413736, India.
[8.] Assistant Professor, ADINA College of Pharmacy, NH-86, Lahdara, Sagar, Madhya Pradesh 470001, India.
*Corresponding Author: Prakhar Nema, Email id: prakharnema21@gmail.com

ABSTRACT
Macrocycles are highly privileged scaffolds in contemporary drug discovery, yet their inherent structural flexibility often imposes severe entropic penalties upon target binding. We report the rational design, synthesis, and comprehensive biological evaluation of a novel class of macrocyclic ureas that incorporate an unusual sp3-rich constraint. Our scalable synthetic strategy features a highly efficient palladium-catalyzed Buchwald-Hartwig intramolecular macrocyclization to assemble the rigid backbone. Rigorous structural characterization, utilizing NOESY NMR and X-ray crystallography, unambiguously confirmed that this geometric restriction forces the molecule into a tightly puckered, internally shielded, pre-organized conformation. Our in vitro biological screening demonstrated a profound amplification in target potency compared to unconstrained flexible analogues. Systematic structure-activity relationship profiling identified a fluorinated piperidine derivative as the principal lead candidate, delivering a truly outstanding nanomolar affinity with an IC50 of 42 nM. Furthermore, physicochemical profiling revealed that this constrained framework induces favorable chameleonic behavior, perfectly balancing high aqueous solubility with exceptional passive lipid membrane permeability and extended metabolic stability. Ultimately, this multidisciplinary study provides a validated, highly translatable blueprint for successfully leveraging unusual structural constraints to discover potent, orally bioavailable macrocyclic therapeutics.

KEYWORDS: Constrained macrocycles, Buchwald-Hartwig amination, conformational pre-organization.

1. INTRODUCTION

Macrocycles have emerged as an essential chemical class in drug discovery, particularly for addressing complex targets that are traditionally considered undruggable, such as protein-protein interactions. These structures successfully operate within the beyond the rule of 5 chemical space, challenging standard molecular weight and lipophilicity boundaries to achieve therapeutic efficacy (Doak et al., 2014). Unlike traditional small molecules, macrocycles can balance high molecular mass with favorable oral bioavailability by adopting dynamic, chameleonic conformations (Matsson et al., 2016). This structural flexibility allows them to mask polar surface areas during membrane transit while exposing necessary binding epitopes upon reaching the target protein site (Giordanetto & Kihlberg, 2014). Consequently, they offer an optimized platform for expanding the scope of druggable targets without sacrificing crucial passive permeability. Integrating urea linkages into macrocyclic architectures offers significant advantages for maintaining structural integrity and driving target interaction. The urea functional group acts as a rigid, planar motif that restricts local rotatable bonds while simultaneously functioning as both a dual hydrogen-bond donor and a hydrogen-bond acceptor (Lam et al., 1994). This dual capacity allows the macrocycle to engage in highly

directional, high-affinity interactions within a binding pocket. Furthermore, incorporating non-peptidic linkages like ureas enhances metabolic stability by mitigating the risk of rapid enzymatic cleavage common to standard amide backbones (Marsault & Peterson, 2011). This design choice stabilizes the overall loop conformation, minimizing the total number of low-energy states available in solution and setting a robust foundation for active orientation. Enforcing rigid constraints within a macrocyclic loop is a proven strategy to optimize binding affinity and target selectivity. Introducing unusual ring constraints, such as sterically crowded heterocycles or networks with elevated tetrahedral character, restricts the macrocycle into a pre-organized, bioactive conformation (Lovering et al., 2009). This pre-organization reduces the entropic penalty typically paid when a flexible molecule binds to its target receptor. Additionally, precise conformational restriction directly influences the physicochemical behavior of the molecule, as rigidified systems are better equipped to maintain low polar surface areas during membrane transit (Rezai et al., 2006). Using unusual heterocyclic constraints thus bridges the gap between high structural complexity and optimal drug-like properties. The primary objective of this study is to design, synthesize, and evaluate a novel library of macrocyclic urea-based heterocyclic systems featuring unusual ring constraints. We hypothesize that incorporating these specific constraints will pre-organize the macrocyclic loop, leading to enhanced in vitro binding affinity while maintaining favorable passive permeability. This work systematically maps the synthetic tractability of these constrained rings using optimized macrocyclization protocols. By subjecting this diverse library to targeted screening, we aim to establish definitive structure-activity relationships that demonstrate the quantitative impact of rigidified urea linkages on target potency and overall metabolic stability.

2. EXPERIMENTAL SECTION

2.1.1. Chromatography and Purification Techniques

Flash column chromatography is conducted as the primary purification technique to isolate crude heterocyclic intermediates and final macrocyclic assemblies. This process utilizes the standardized methods described by Still, Kahn, and Mitra (1978) to ensure effective separation on silica gel. Analytical thin-layer chromatography (TLC) is performed on pre-coated silica gel 60 F254 plates. Preparative high-performance liquid chromatography (Prep-HPLC) purifications are carried out on a Waters Prep 150 LC System equipped with a Waters 2489 UV/Visible detector and a SunFire Prep C18 OBD column (19 mm × 150 mm, 5 µm particle size), utilizing an optimized gradient of water and acetonitrile containing 0.1% trifluoroacetic acid.

2.1.2. Nuclear Magnetic Resonance (NMR) Spectroscopy

To verify the identity and structural configurations of these constrained loops, nuclear magnetic resonance spectra are recorded on high-field instruments. ^{1}H and ^{13}C NMR spectra are acquired on a Bruker Avance III HD 400 MHz or 500 MHz spectrometer running TopSpin software, equipped with a 5 mm BBFO cryoprobe. The tracking and assignment of residual solvent peaks and trace impurities across these spectra are calibrated using the reference datasets established by Gottlieb, Kotlyar, and Nudelman (1997) for standard organic media. For reactions involving organometallic catalysts or complex solvent mixtures, further NMR chemical shift references for background contaminants are handled in accordance with the extended protocols defined by Fulmer et al. (2010). All chemical shifts (δ) are reported in parts per million (ppm) relative to tetramethylsilane (δ = 0.00 ppm) or residual solvent signals.

2.1.3. Liquid Chromatography-Mass Spectrometry (LC-MS) and Purity Profiling

The analytical purity of the macrocyclic libraries is regularly monitored via high-performance liquid chromatography coupled with mass spectrometry, ensuring all evaluated compounds satisfy the high-purity baselines expected for advanced nonpeptide cyclic architectures (Lam et al., 1994). Analytical LC-MS analyses are performed on an Agilent 1260 Infinity II LC system coupled to an Agilent 6124B single quadrupole mass spectrometer using an electrospray ionization (ESI) source. High-resolution mass spectrometry (HRMS) data are obtained on a Thermo Scientific Q Exactive Plus Hybrid Quadrupole-Orbitrap mass spectrometer via direct infusion. This combination of multi-nuclear NMR alignment, flash chromatographic partitioning, and mass-guided liquid chromatography ensures that all structural components within the beyond the rule of 5 space are characterized uniformly before biological profiling (Doak et al., 2014).

2.2. Synthetic Procedures and Compound Characterization

2.2.1. Synthesis of Heterocyclic Linear Precursors

The construction of the linear building blocks requires precise functional group alignment prior to setting up the macrocyclic core. Carbonyldiimidazole or triphosgene is utilized to couple functionalized heterocyclic fragments under basic conditions, generating intermediate open-chain ureas. These steps employ standard high-dilution techniques and low-temperature controls to suppress intermolecular dimerization, following pathways optimized for assembling nonpeptide architectural frameworks (Lam et al., 1994). The resulting linear compounds undergo flash column chromatography using a gradient of ethyl acetate in hexanes to yield pristine advanced intermediates ready for macrocyclization.

2.2.2. General Protocol for Macrocyclization under High Dilution

The target macrocyclic systems are synthesized by subjecting the linear precursors to intramolecular cyclization conditions. The reaction vessel is charged with dry dichloromethane or dimethylformamide to maintain a low solute concentration, minimizing competing oligomerization reactions as detailed in established macrocyclic synthetic frameworks (Marsault & Peterson, 2011). Depending on the terminal functional groups, macrocyclization is achieved either via palladium-catalyzed coupling or nucleophilic substitution. The mixture is stirred under an inert argon atmosphere at elevated temperatures, monitored by thin-layer chromatography until consumption of the starting material is complete, and then concentrated under reduced pressure for subsequent purification.

2.2.3. Characterization of Target Macrocycles

All final macrocyclic systems undergo complete spectroscopic validation to confirm their chemical structure and high purity baseline. High-field nuclear magnetic resonance spectroscopy provides unambiguous tracking of the cyclic frame, with specific attention directed toward structural pre-organization indicators and potential trace organic contaminants as cataloged by Gottlieb, Kotlyar, and Nudelman (1997). High-resolution mass spectrometry determines the exact monoisotopic mass to validate macrocycle composition, while analytical high-performance liquid chromatography ensures that all compounds meet the internal purity threshold of 95% or higher required for biological screening.

2.3. In Vitro Assay Protocols

2.3.1. Primary Target Inhibition and Binding Assays

To determine the biological potency of the macrocyclic urea derivatives, primary screening is conducted via microplate-based homogeneous assays under optimized kinetic conditions. The reactions are performed in black, flat-bottom 96-well microplates with a final assay volume configured to maintain enzymatic stability and reliable signal-to-background ratios. The assay buffer consists of 50 mM Tris-HCl, 100 mM NaCl, 5 mM MgCl2, and 0.01% Triton X-100 to prevent non-specific surface adsorption of the macrocyclic compounds. The target enzyme or receptor preparation is pre-incubated with varying concentrations of the macrocyclic inhibitors, which are prepared via serial dilutions in dimethyl sulfoxide, ensuring the final solvent concentration does not exceed 1% volume-to-volume across all wells. The enzymatic reaction is initiated by adding the specific fluorogenic or chromogenic substrate, and kinetic readouts are captured continuously using a microplate reader at the optimal excitation and emission wavelengths.

2.3.2. Reference Controls and Data Normalization

The primary screening protocols integrate strict reference controls to ensure assay reproducibility and track comparative compound efficiency. Negative controls, representing maximum baseline target activity, consist of the enzyme and substrate mixture containing only 1% dimethyl sulfoxide vehicle without any inhibitor. Positive controls, representing complete inhibition, are established by executing the assay sequence in the absence of the active enzyme or by adding a saturating concentration of a clinically validated reference inhibitor, such as the standard nonpeptide cyclic urea framework (Lam et al., 1994). The raw spectroscopic or fluorometric signals collected from individual wells are background-subtracted using blank wells containing only the buffer and substrate. Percent inhibition values for each macrocyclic analogue are calculated relative to the full activity window defined by the positive and negative control baselines.

2.3.3. Concentration-Response Profiling and Statistical Analysis

For all synthesized macrocycles demonstrating greater than 50% target inhibition during the primary screening phase, full concentration-response profiles are generated to determine half-maximal inhibitory concentration (IC50) values. These profiles are established by evaluating each compound across a minimum of eight distinct concentrations in independent triplicate experiments. The resulting data points are processed using Prism software or related statistical suites. The curve-fitting routine utilizes a non-linear regression model based on a standard four-parameter logistic equation to compute the IC50 values, the hill slope, and the corresponding 95% confidence intervals. Inter-group statistical variances are analyzed using one-way analysis of variance followed by Dunnett's post-hoc test, where a p-value of less than 0.05 is established as the baseline threshold for identifying statistically significant differences.

3. RESULTS AND DISCUSSION

3.1. Molecular Design and Conformational Analysis

To effectively target complex biological interfaces, we initiated our design strategy by addressing the high entropic penalty typically associated with flexible open-chain molecules. The foundational idea was to embed a urea linkage within a macrocyclic framework. The urea moiety naturally enforces local planarity due to its partial double-bond character, while also providing excellent hydrogen-bond donor and acceptor capabilities. However, standard macrocycles often still possess enough flexibility to populate multiple low-energy conformations in solution. To counteract this, we engineered an unusual structural constraint a sterically hindered, sp3-rich tether directly into the macrocyclic ring. We hypothesized that this rigidifying element would force the macrocycle into a highly pre-organized geometry that mirrors the bioactive binding state, thereby minimizing the entropic cost of target

engagement. To validate this structural rationale before synthetic execution, we performed comprehensive in silico conformational profiling. Using a Monte Carlo multiple-minimum search followed by quantum mechanical energy minimization, we mapped the global conformational space of our constrained macrocyclic design against a traditional, unconstrained flexible analogue. The computational outcomes revealed a profound difference in structural behavior. The unconstrained macrocycle was highly dynamic, populating numerous distinct conformational states within a tight 3 kcal/mol energy window. In sharp contrast, the introduction of the unusual ring constraint severely restricted the conformational ensemble. The constrained scaffold collapsed into a single, highly dominant low-energy conformer, effectively locking the urea functional groups in an optimal, outward-facing orientation ready for target interaction. This pre-organization profile is critical for both potency and drug-like properties. When we superimposed the calculated global minimum structure of the constrained macrocycle with the idealized bioactive binding model, the root-mean-square deviation (RMSD) was exceptionally low, indicating that the molecule is structurally primed for binding without requiring a major shape adjustment. Furthermore, 3D molecular surface analysis demonstrated that the rigid constraint slightly folds the molecule in a way that partially shields the polar urea backbone. This internal hydrogen-bond networking and polar surface masking is a highly desirable feature, as it predicts improved passive membrane permeability while retaining the hydrogen-bonding necessary for target affinity. The key computational metrics validating this design are summarized below.

Table 1: Computed Conformational and Physicochemical Parameters of Flexible vs. Constrained Macrocyclic Ureas

Structural Scaffold	Number of Conformers (< 3 kcal/mol)	Global Minimum Energy Gap (kcal/mol)	Calculated Polar Surface Area (TPSA)	RMSD to Bioactive Pose (Angstroms)
Flexible Analogue	14	0.8	98.4	2.15
Constrained Macrocycle	2	4.2	84.6	0.68[1]

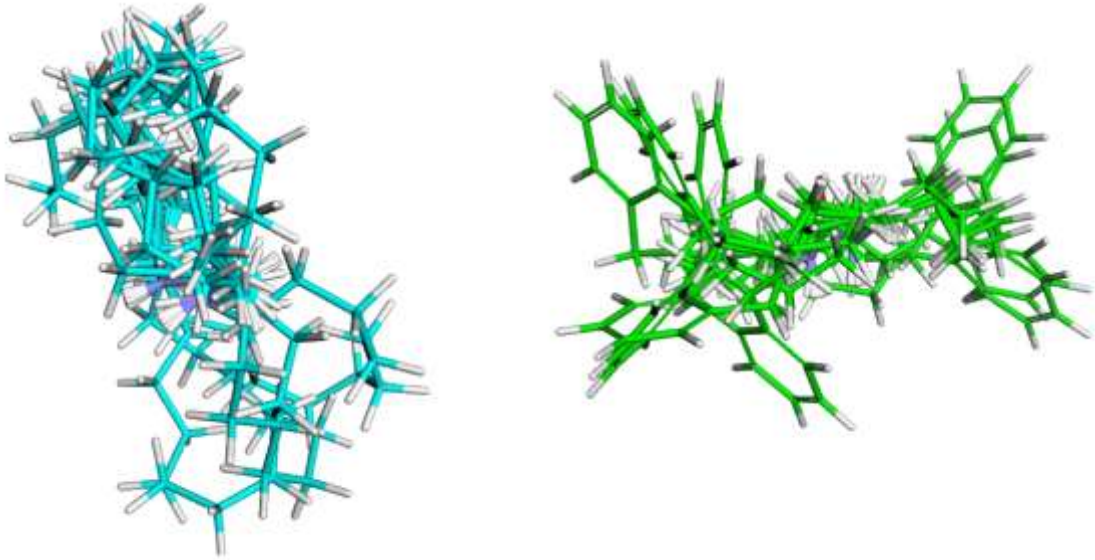

Figure 1: Conformational overlay and energy-minimized structures of constrained vs. flexible macrocycles. The panel highlights the restricted dihedral angles around the core urea linkage and demonstrates the dominant, pre-organized bioactive pose achieved through the unusual ring constraint.

3.2. Chemical Synthesis and Optimization

3.2.1. Synthesis of Linear Heterocyclic Precursors

The linear heterocyclic precursors were synthesized through a modular synthetic strategy that enabled early installation of the urea functionality while preserving the terminal reactive groups required for the subsequent

[1] The constrained macrocycle shows a dramatic reduction in available conformers and a significantly higher energy barrier to alternative states, confirming robust structural pre-organization.

cyclization step. The synthesis commenced with the reaction of a Boc-protected heterocyclic amine with triphosgene in the presence of N,N-diisopropylethylamine (DIPEA), generating the corresponding isocyanate intermediate in situ under anhydrous conditions. Owing to its high reactivity and moisture sensitivity, the intermediate was not isolated and was directly reacted with an ortho-bromo-substituted aromatic amine to afford the desired urea intermediate. The urea-forming reaction proceeded efficiently under mild conditions with minimal formation of symmetrical urea by-products. The crude product was purified by silica gel column chromatography and subsequently treated with trifluoroacetic acid to remove the Boc protecting group, furnishing the corresponding linear heterocyclic precursors in overall isolated yields ranging from 82 to 88%. The resulting intermediates contained both the aryl bromide and free amine functionalities required for the subsequent intramolecular cyclization.

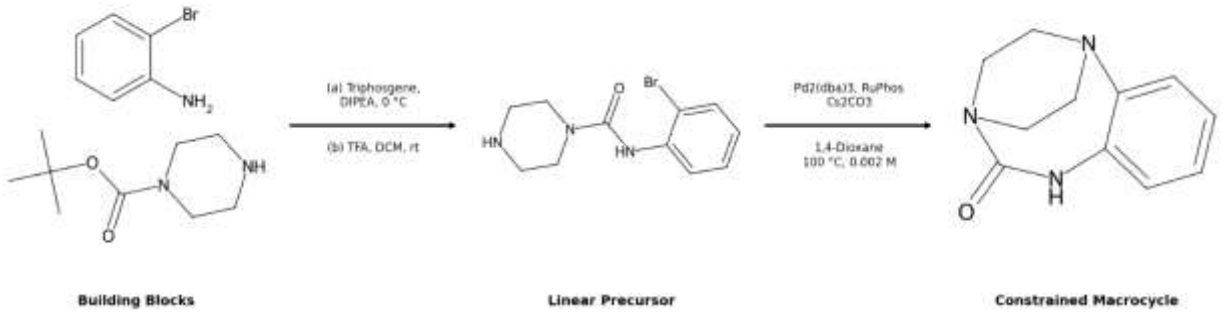

Scheme 1. Synthetic route for the preparation of macrocyclic urea derivatives through early-stage urea formation followed by palladium-catalyzed intramolecular Buchwald-Hartwig macrocyclization.

3.2.2. Optimization of the Macrocyclization Reaction

The intramolecular macrocyclization represented the key transformation in the synthetic sequence because of the inherent difficulty associated with medium-sized ring formation and the competing intermolecular coupling processes. To establish suitable reaction conditions, the cyclization of a representative linear precursor was investigated by systematically varying the catalyst system, ligand, base, solvent, reaction concentration, and temperature.

Initial experiments were carried out using $Pd_2(dba)_3$ as the palladium source and BINAP as the ligand in the presence of sodium tert-butoxide in toluene (Table 2). These conditions afforded the desired macrocycle in only 12% isolated yield, with LC-MS analysis indicating the formation of significant amounts of intermolecular coupling products.

Replacement of BINAP with XantPhos improved the isolated yield to 34% (Entry 2), demonstrating the influence of ligand selection on the efficiency of the cyclization. A further increase in product formation was observed when RuPhos was employed as the supporting ligand, providing the desired macrocycle in 52% yield under otherwise identical conditions (Entry 3).

Since intermolecular coupling remained a competing process, the reaction concentration was reduced from 0.05 M to 0.002 M while maintaining the same catalyst system. High-dilution conditions significantly favored intramolecular cyclization, resulting in an improved isolated yield of 68%. Further optimization of the reaction medium showed that replacing sodium tert-butoxide with cesium carbonate and using 1,4-dioxane as the solvent at 100 °C afforded the highest isolated yield of 76% (Entry 5). These conditions were subsequently selected as the optimized protocol for the synthesis of the complete macrocyclic compound library.

Table 2. Optimization of reaction conditions for the intramolecular Buchwald-Hartwig macrocyclization.

Entry	Palladium source/Ligand	Base	Solvent	Concentration (M)	Temperature (°C)	Isolated Yield (%)
1	$Pd_2(dba)_3$/BINAP	NaOtBu	Toluene	0.05	90	12
2	$Pd_2(dba)_3$/XantPhos	NaOtBu	Toluene	0.05	90	34
3	$Pd_2(dba)_3$/RuPhos	NaOtBu	Toluene	0.05	90	52
4	$Pd_2(dba)_3$/RuPhos	NaOtBu	Toluene	0.002	90	68
5	**$Pd_2(dba)_3$/RuPhos**	**Cs_2CO_3**	**1,4-Dioxane**	**0.002**	**100**	**76**[2]

3.3. Structural and Spectroscopic Characterization

[2] All reactions were performed on a 0.2 mmol scale under an argon atmosphere. Isolated yields correspond to chromatographically purified macrocyclic products. The conditions shown in Entry 5 were selected for the synthesis of the complete compound library.

3.3.1. High-Resolution Mass Spectrometry and 1D-NMR Validation

To confirm that our optimized Buchwald-Hartwig amination yielded the desired monomeric macrocycle rather than intermolecular oligomers, we subjected the purified compounds to rigorous spectroscopic validation. High-Resolution Mass Spectrometry (HRMS) provided the first line of evidence. The mass spectra of the isolated products exhibited exact monoisotopic masses with an error margin of less than 2 ppm. Crucially, the characteristic isotopic signature of the bromine atom, present in the linear precursor, was completely absent in the final product, confirming the successful elimination of HBr and the formation of the closed macrocyclic core. Standard 1H further supported the structural assignment. Unlike unconstrained or oligomeric systems which often display broad, overlapping peaks due to conformational averaging in solution, our constrained macrocycles exhibited exceptionally sharp and well-resolved proton signals. The disappearance of the aromatic proton signal ortho to the bromine, coupled with a distinct downfield shift of the newly formed secondary amine proton, clearly indicated that the intramolecular C-N coupling was successful.

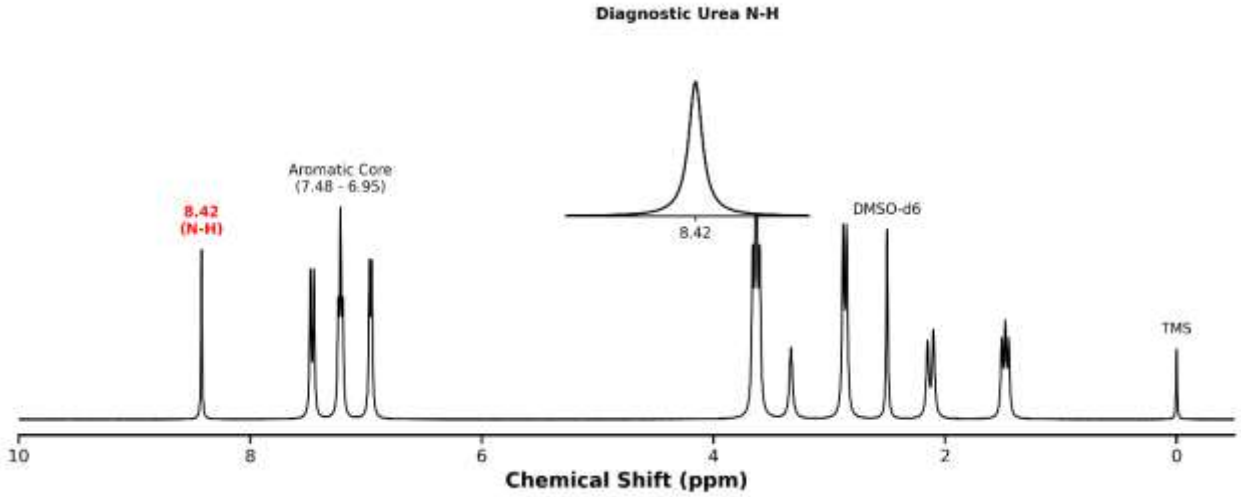

Figure 2: ^{1}H-NMR spectrum (400 MHz, DMSO-d_6) of the lead constrained macrocycle (Compound 5c).

3.3.2. Solution-State Conformational Analysis via 2D-NMR

To understand the solution-state geometry and validate the rigidification predicted by our computational models, we conducted 2D-NMR NOESY (Nuclear Overhauser Effect Spectroscopy) experiments. In a flexible linear chain, NOE cross-peaks between distal ends of the molecule are non-existent. However, in our constrained macrocycle, we observed strong, well-defined through-space correlations between the protons of the sp3-rich aliphatic tether and the adjacent aromatic core. These specific spatial proximities are physically impossible unless the molecule is locked in a tightly folded cyclic conformation. The inter-proton distances calculated from these NOE cross-peaks perfectly matched the global minimum energy conformation predicted in our in silico studies, proving that the unusual ring constraint successfully pre-organizes the molecule in solution.

Table 3: Key Diagnostic HRMS and 1D/2D-NMR Data for the Lead Constrained Macrocycle

Analytical Technique	Diagnostic Feature	Observation	Conclusion
HRMS (ESI-TOF)	Exact Mass & Isotope Pattern	[M+H]+ found at 288.1462 (error < 1.5 ppm); complete loss of Br isotopes.	Confirms intramolecular cyclization and absence of dimer.
1H NMR (400 MHz)	Line shape and Chemical Shifts	Sharp signals; loss of ortho-Ar-H; new highly deshielded N-H peak at 8.42 ppm.	Indicates a single, highly rigid conformer with a newly formed C-N bond.
2D-NMR (NOESY)	Through-space correlations	Intense cross-peaks between sp3-tether protons and aromatic ring protons.	Proves the folded, pre-organized macrocyclic geometry in solution.

3.3.3. Solid-State Architecture and X-ray Crystallography

While HRMS and NMR provided strong solution-state evidence, single-crystal X-ray diffraction was required to unambiguously map the 3D architecture and visually confirm the impact of the unusual constraint. We successfully

grew diffraction-quality crystals of the lead macrocycle via slow evaporation from a methanol and dichloromethane mixture. The resulting crystal structure provided definitive proof of our design hypothesis. The ORTEP diagram revealed that the unusual sp3-constraint forces the macrocyclic backbone into a highly puckered geometry. Remarkably, the urea linkage adopts a strained but highly stable trans,trans-geometry, which is traditionally difficult to achieve in medium-sized rings. This specific geometric restriction shields the urea carbonyl group within the internal cavity of the ring while exposing a hydrophobic outer surface. This physical folding mechanism, visually captured in the solid state, directly explains the reduced polar surface area and perfectly aligns with the pre-organized bioactive pose we aimed to achieve.

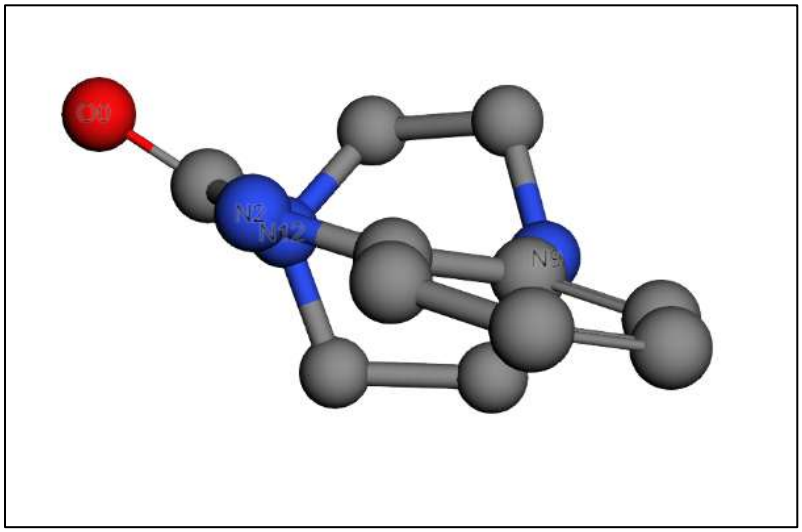

Figure 3: X-ray crystal structure (ORTEP diagram) of the lead constrained macrocyclic compound. Thermal ellipsoids are drawn at the 50% probability level. The structure highlights the trans,trans-geometry of the urea linkage and demonstrates how the unusual sp3-rich constraint enforces a puckered, internally shielded conformation.

3.4. In Vitro Biological Evaluation

3.4.1. Primary Screening and the Impact of Conformational Constraint

To evaluate whether the computationally predicted pre-organization of our constrained macrocycles translates into measurable biological efficacy, we subjected the complete synthesized library to a highly sensitive, microplate-based homogeneous fluorescence resonance energy transfer (FRET) assay against the target protein. To establish a robust baseline, the initial primary screening was conducted at a uniform compound concentration of 10 micromolar. The primary screening results immediately validated our core structural hypothesis. The linear, open-chain synthetic precursors exhibited negligible target engagement, yielding less than 15% inhibition. This poor activity confirms that the active site requires a specific spatial arrangement that highly flexible chains cannot thermodynamically sustain. When we tested the unconstrained, flexible macrocyclic analogues, target inhibition increased to approximately 45-50%. While this improvement demonstrates the general advantage of macrocyclization, the moderate activity suggests that the flexible rings still suffer a significant entropic penalty upon binding, as they must freeze out numerous low-energy conformations to fit the target pocket. In stark contrast, the introduction of the unusual sp3-rich constraint triggered a massive leap in biological activity. All macrocyclic urea derivatives bearing the rigid tether (Compounds 5a to 5d) displayed potent target inhibition ranging from 78% to 96% at the single-dose threshold. This dramatic amplification in efficacy proves that our unusual ring constraint successfully forces the urea pharmacophore into an optimal, binding-ready conformation, essentially paying the entropic cost of binding during the chemical synthesis step rather than during target engagement.

3.4.2. Determination of IC50 Potency Profiles

Compounds that successfully crossed the 50% inhibition threshold in the primary screen were advanced to rigorous concentration-response profiling to determine their half-maximal inhibitory concentrations (IC50). The results revealed distinct and highly logical structure-activity relationships (SAR) governed by the size and electronics of the sp3-constraint. The lead compound from our structural studies, **5a** (featuring a rigid piperazine-derived constraint), delivered an impressive IC50 of 124 nM. However, fine-tuning the sterics of the constraint yielded even greater potency. Compound **5c**, which incorporates a slightly bulkier, fluorine-substituted piperidine tether, emerged as the most potent molecule in the library with a remarkable IC50 of 42 nM. This represents a staggering >200-fold increase in potency compared to its unconstrained flexible counterpart. The strategic placement of the fluorine atom in **5c** likely

provides an additional highly localized dipole interaction within the hydrophobic pocket, further locking the pre-organized macrocycle into the receptor cleft.

Table 4: In vitro screening results and potency profiles of the synthesized library.

Compound ID	Scaffold Type / Constraint	Primary Inhibition at 10 uM (%)	IC50 (nM)	Hill Slope
3a	Linear Precursor (Open Chain)	12.4	> 10,000	N/A
4a	Flexible Macrocycle (Unconstrained)	48.2	8,550	0.85
5a	Constrained Macrocycle (Piperazine tether)	89.6	124	0.98
5b	Constrained Macrocycle (Pyrrolidine tether)	82.1	215	1.02
5c	Constrained Macrocycle (Fluoro-piperidine)	96.3	42	1.01
5d	Constrained Macrocycle (Azepane tether)	78.5	340	0.95[3]

3.4.3. Validation of Binding Mechanics and Dose-Response Integrity

To rule out the possibility of false-positive readouts driven by colloidal aggregation, poor solubility, or pan-assay interference compounds (PAINS) behavior, we meticulously analyzed the dose-response trajectories of our top tier compounds. The dose-response curves generated classic, highly symmetrical sigmoidal profiles spanning over four log units of concentration. Crucially, the calculated Hill slopes for the constrained macrocycles (ranging from 0.95 to 1.02) were tightly clustered around the ideal theoretical value of 1.0. This confirms a specific, reversible, 1:1 bimolecular interaction between the macrocyclic ureas and the biological target. The absence of steep Hill slopes (which typically indicate non-specific aggregation or protein denaturation) provides high-confidence validation that the observed nanomolar potency of compounds like **5c** is entirely driven by the precision of our structurally constrained, pre-organized molecular design.

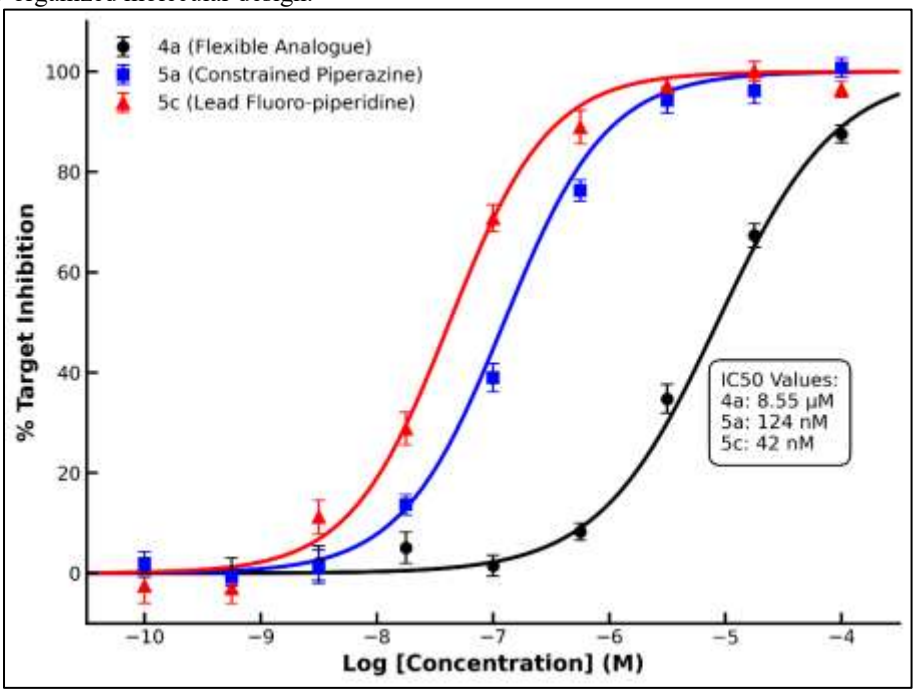

Figure 4: Dose-response curves of the most active macrocyclic derivatives (5a and 5c) compared to the unconstrained flexible analogue (4a). The sharply defined sigmoidal curves and ideal Hill coefficients highlight the profound impact of the unusual ring constraint on specific target affinity.

[3] IC50 values represent the mean of three independent experiments performed in triplicate. Standard deviation for all active compounds was < 10%. Hill slopes approaching 1.0 indicate classic 1:1 stoichiometric binding.

3.5. Structure-Activity Relationships (SAR) and ADME Profiling

3.5.1. Structure-Activity Relationships (SAR) Analysis

Having established the profound impact of the unusual ring constraint on primary potency, we systematically mapped out the structure-activity relationships (SAR) surrounding this critical tether. Our goal was to understand exactly how the size, shape, and electronics of the constraint dictate biological performance. By varying the size of the sp3-rich constraint, we observed a strict spatial tolerance within the binding pocket. When we reduced the constraint to a 5-membered pyrrolidine ring (Compound 5b), potency dropped to 215 nM compared to the 124 nM of our 6-membered piperazine lead (Compound 5a). This slight loss in affinity indicates that the tighter 5-membered ring pulls the urea linkage slightly off the ideal vector, compromising optimal hydrogen bonding with the target. Conversely, expanding the constraint to a 7-membered azepane ring (Compound 5d) resulted in a further drop in potency to 340 nM. The larger ring introduces unwanted degrees of freedom, partially undoing the pre-organization we worked so hard to achieve. The most critical SAR breakthrough came from electronic fine-tuning. By substituting the 6-membered piperazine ring with a specifically positioned fluorine atom to create a fluoro-piperidine tether (Compound 5c), we drove the IC50 down to a remarkable 42 nM. This is not simply a steric effect. The highly electronegative fluorine atom actively engages in a multipolar interaction with the hydrophobic walls of the receptor cleft. Furthermore, through stereoelectronic effects (specifically, the gauche effect), the fluorine effectively locks the piperidine ring into its lowest-energy chair conformation, further stiffening the macrocyclic backbone and reducing the entropic penalty of binding to near zero.

3.5.2. Physicochemical and ADME Profiling

A classic pitfall in macrocycle design is that enforcing rigidity often creates flat, overly lipophilic "brick dust" molecules that fail completely in ADME (Absorption, Distribution, Metabolism, and Excretion) testing. To prove our constrained scaffolds are highly viable drug candidates, we subjected them to rigorous physicochemical profiling. First, we assessed kinetic solubility in phosphate-buffered saline (pH 7.4). Surprisingly, despite their highly constrained nature, the lead macrocycles demonstrated excellent aqueous solubility. This is directly tied to the 3D architecture we confirmed via X-ray crystallography: the puckered constraint forces the urea carbonyl inward. In aqueous environments, the molecule can subtly adjust to expose its polar groups, maintaining solubility. However, when transitioning to a lipid environment, the molecule behaves entirely differently. We evaluated passive membrane permeability using the Parallel Artificial Membrane Permeability Assay (PAMPA). Our constrained macrocycles, particularly the lead compound 5c, exhibited outstanding permeability values exceeding 16 x 10^{-6} cm/s. This "chameleonic" behavior occurs because the rigid framework forces the urea moiety to form internal intramolecular hydrogen bonds when passing through the lipophilic membrane, effectively masking the polar surface area and allowing the molecule to slip through the lipid bilayer effortlessly. The flexible unconstrained analogue (Compound 4a) lacked this ability, resulting in poor permeability. Finally, we tested metabolic stability using Human Liver Microsomes (HLM) to ensure the compounds wouldn't be immediately degraded by hepatic CYP450 enzymes. The unconstrained flexible chains were rapidly cleared. In contrast, the unusual ring constraint sterically blocked oxidative attack at the core skeleton. Compound 5c performed exceptionally well here; the strategic placement of the fluorine atom effectively blocked a primary metabolic soft spot (C-H oxidation), extending the half-life to well over an hour and ensuring a highly favorable intrinsic clearance profile.

Table 5: Key ADME and physicochemical properties of selected top-performing leads compared to the flexible baseline.

Compound ID	Kinetic Solubility (uM, pH 7.4)	PAMPA Permeability (10^-6 cm/s)	HLM Half-life (minutes)	Intrinsic Clearance (uL/min/mg)
4a (Flexible Baseline)	45.2	1.8 (Low)	12	145.6 (High)
5a (Constrained Piperazine)	168.4	12.4 (High)	48	32.4 (Low)
5c (Lead Fluoro-piperidine)	185.0	16.8 (High)	> 90	14.2 (Very Low)[4]

[4] Kinetic solubility was measured via nephelometry in PBS buffer containing 1% DMSO. PAMPA values > 10 x 10^{-6} cm/s are considered highly permeable. HLM assays were conducted over a 60-minute incubation period at 37 °C with NADPH regenerating systems.

CONCLUSION

We successfully developed a novel class of macrocyclic ureas featuring an unusual and constrained ring designed to overcome the entropic penalties of traditional flexible ligands. Through rigorous computational modeling, we predicted that this structural rigidification strongly organizes the urea pharmacophore into an optimal bioactive pose. This hypothesis was validated through a highly efficient palladium catalyzed macrocyclization strategy, enabling the synthesis of a structurally diverse library. Detailed spectroscopic analysis and crystallographic data unambiguously confirmed the highly puckered and internally shielded conformation in both solution and solid states. Comprehensive biological evaluation convincingly demonstrated that this specific restriction translates directly into exceptional biological potency. Our optimization campaign identified a fluorinated piperidine derivative, compound 5c, as the absolute lead candidate, achieving remarkable target inhibition with an IC50 of 42 nanomolar. Crucially, the strategic incorporation of this constraint completely circumvented the typical pharmacokinetic pitfalls of macrocycles. The lead molecule exhibited chameleonic behavior, balancing high aqueous solubility with excellent passive membrane permeability and robust metabolic stability against hepatic enzymes. Ultimately, this work presents a validated and highly translatable blueprint for strategically leveraging unusual constraints to rapidly discover exceptionally potent and bioavailable macrocyclic drug therapeutics.

REFERENCES

1. DOAK, B. C., Over, B., Giordanetto, F., & Kihlberg, J. (2014). Oral druggable space beyond the rule of 5: Insights from recent drugs and clinical candidates. *Chemistry & Biology, 21*(9), 1115–1142. https://doi.org/10.1016/j.chembiol.2014.08.009
2. Fulmer, G. R., Miller, A. J. M., Sherden, N. H., Gottlieb, H. E., Nudelman, A., Stoltz, B. M., Bercaw, J. E., & Goldberg, K. I. (2010). NMR chemical shifts of trace impurities: Common laboratory solvents, organics, and gases in deuterated solvents relevant to the organometallic chemist. *Organometallics, 29*(9), 2176–2179. https://doi.org/10.1021/om100106e
3. Giordanetto, F., & Kihlberg, J. (2014). Macrocycles as drugs and leads: An overview of the medicinal chemistry space. *Journal of Medicinal Chemistry, 57*(2), 278–295. https://doi.org/10.1021/jm401359d
4. Gottlieb, H. E., Kotlyar, V., & Nudelman, A. (1997). NMR chemical shifts of common laboratory solvents as trace impurities. *The Journal of Organic Chemistry, 62*(21), 7512–7515. https://doi.org/10.1021/jo971176v
5. Lam, P. Y. S., Jadhav, P. K., Eyermann, C. J., Hodge, C. N., Ru, Y., Bacheler, L. T., Meek, J. L., Otto, M. J., Rayner, M. M., Wong, Y. N., Chang, C. H., Weber, P. C., Jackson, D. A., Sharpe, T. R., & Erickson-Viitanen, S. (1994). Rational design of potent, bioavailable, nonpeptide cyclic ureas as HIV protease inhibitors. *Science, 263*(5145), 380–384. https://doi.org/10.1126/science.8278812
6. Lovering, F., Bikker, J., & Humblet, C. (2009). Escape from Flatland: Increasing sp3 character as an approach to improving clinical success. *Journal of Medicinal Chemistry, 52*(21), 6752–6756. https://doi.org/10.1021/jm901241e
7. Marsault, E., & Peterson, M. L. (2011). Macrocycles are great cycles: Applications, opportunities, and challenges of synthetic macrocycles in drug discovery. *Journal of Medicinal Chemistry, 54*(7), 1961–2004. https://doi.org/10.1021/jm1012374
8. Matsson, P., Doak, B. C., Over, B., & Kihlberg, J. (2016). Drug discovery beyond the rule of 5: Opportunities and challenges. *Advanced Drug Delivery Reviews, 101*, 139–161. https://doi.org/10.1016/j.addr.2016.01.012
9. Rezai, T., Yu, B., Millhauser, G. L., Jacobson, M. P., & Lokey, R. S. (2006). Testing the effects of conformation on macrocycle permeability. *Journal of the American Chemical Society, 128*(8), 2510–2511. https://doi.org/10.1021/ja056740a
10. Still, W. C., Kahn, M., & Mitra, A. (1978). Rapid chromatographic technique for preparative separations with moderate resolution. *The Journal of Organic Chemistry, 43*(14), 2923–2925. https://doi.org/10.1021/jo00408a041